

Spin-Resolved Mapping of Spin Contribution to Exchange-Correlation Holes

F. O. Schumann, C. Winkler, and J. Kirschner

Max-Planck Institut für Mikrostrukturphysik, Weinberg 2, 06120 Halle, Germany

F. Giebels, H. Gollisch, and R. Feder

Theoretische Festkörperphysik, Universität Duisburg-Essen, 47048 Duisburg, Germany

(Received 10 November 2009; published 26 February 2010)

By means of spin-polarized electron coincidence spectroscopy we explore the fundamental issue of spin-resolved contributions to the exchange-correlation hole in many-electron systems. We present a joint experimental and theoretical study of correlated electron pair emission from a ferromagnetic Fe(001) surface induced by spin-polarized low-energy electrons. We demonstrate that the contribution to the exchange-correlation hole due to exchange is more extended than the contribution due to the screened Coulomb interaction.

DOI: [10.1103/PhysRevLett.104.087602](https://doi.org/10.1103/PhysRevLett.104.087602)

PACS numbers: 79.60.-i, 73.20.At

In seminal papers Wigner & Seitz [1] and Slater [2] introduced the concept of the exchange-correlation (xc) hole in many-electron systems. This is defined in real space and is closely related to the pair correlation function. The essential point is that around each electron the electronic charge density is reduced such that the charge deficit amounts to exactly one elementary charge. This result is a combination of two effects, namely, the Pauli principle and the repulsive Coulomb interaction. The Pauli principle demands that two electrons with parallel spins can not be at the same location, while the Coulomb correlation will force electrons to stay apart independent of the spin orientation. The extension of the exchange part and correlation part of the xc hole do not have to be necessarily the same. Slater discussed these differences in the pair correlation function [2]. For parallel spins both exchange and Coulomb interaction play a role, while antiparallel spin electrons experience only the Coulomb interaction. The region of reduced charge density is larger for parallel spins than for antiparallel spins. The concept of the xc hole is of pivotal importance in modern solid state theory, because it determines the exchange-correlation energy term which is a central part within density functional theory. There are currently intense efforts underway to improve the accuracy of the exchange-correlation term. The importance of this term becomes clear if we recall that it contains essential many-body effects, e.g., magnetism.

It would be interesting to perform experiments aimed to separate the relative size and magnitude of the exchange and correlation contribution to the xc hole. An experimental approach, which is sensitive to the electron-electron interaction, is the electron pair emission from surfaces excited by a sufficiently energetic primary electron. It has been demonstrated that the concept of the xc hole can be studied by the electron pair emission from surfaces. The xc hole manifests itself through a reduction of the pair emission intensity around the fixed emission direction of one electron, which we may call the depletion zone [3–8].

We learn from this that the minimum of the momentum distribution correlates with the minimum of the pair correlation function. One may speculate whether a spin dependence can be observed in the momentum distribution. For this one needs to be able to adjust the relative spin orientation of the incoming electron and the target electron. In this way it is possible to “switch off” the contribution due to exchange. The generation of a spin-polarized primary beam is an established technique [9–11]. Spin-polarized target electrons are available in ferromagnets, where the overall population of one spin direction (called majority) is larger than for the opposite spin direction (called minority). The orientation of the majority direction can be controlled via an external magnetic field. To maximize the spin dependence of the observable momentum distribution, one needs energy and momentum conditions, for which target electrons with one spin orientation strongly predominate. We find such conditions by means of an *ab initio* electronic structure calculation. By experiment and corresponding pair emission theory we provide the first demonstration that it is possible to disentangle exchange and correlation. We observe that the depletion zone for exchange is larger than for correlation.

We built a time-of-flight (TOF) coincidence apparatus using a spin-polarized primary beam and a ferromagnetic sample; see Fig. 1. A spin-polarized electron beam is created via photoemission with circular polarized light from a GaAs surface [9–11]. Switching the light helicity reverses the polarization direction. This spin-polarized primary beam hits the sample along the surface normal. In our coordinate system the x and y axis are in the surface plane. Two channelplate detectors (labeled “left” and “right”) with delay line anodes allow the determination of the impact positions of the electrons. A coincidence circuit ensures that only one electron pair per incident electron pulse is detected. From the flight time and the impact position we determine the kinetic energy and the in-plane components of the momentum for each electron. The

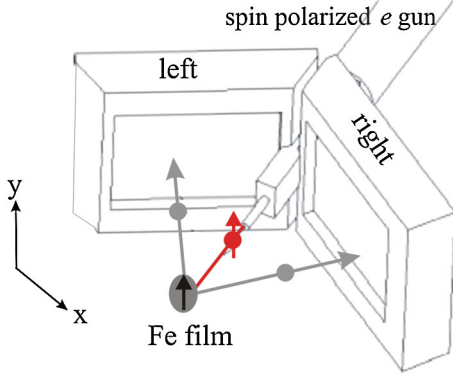


FIG. 1 (color). A transversely spin-polarized electron hits a ferromagnetic sample. The relative orientation of the majority and polarization direction can be independently reversed. Momentum distributions are obtained via position sensitive detectors and time-of-flight analysis.

kinetic energy is defined with respect to the vacuum level. We grow an approximately 20 ML thick Fe film on a W(001) surface. It is magnetized in-plane with the easy axis along the [010] direction which is parallel to the y axis; see Fig. 1. We can apply a pulsed magnetic field along the y axis for reversing the magnetization. The spin polarization of the incoming beam is also along the y axis. The primary spin polarization and majority spin direction can be individually controlled. Therefore, the observed spectra can be grouped into two subsets: (i) for subset I^+ primary spin and majority spin directions are parallel (ii) events with antiparallel alignment of primary electron and majority spin are contained in subset I^- . The reversal of the relative spin orientation occurred every few minutes. The data acquisition times for both spin alignments are equal allowing direct comparison of the intensity levels. The total acquisition time was a few months due to the requirement to operate at low primary flux. This is mandatory in order to reduce the detection from two electrons in coincidence which come from different primary electrons. Our target is a single crystalline surface therefore the in-plane component of the momentum must be conserved (modulo a reciprocal surface lattice vector). This can be written as

$$\mathbf{k}_{\parallel}^v + \mathbf{k}_{\parallel}^p = \mathbf{k}_{\parallel}^l + \mathbf{k}_{\parallel}^r = \mathbf{k}_{\parallel}^{\text{sum}}. \quad (1)$$

On the left side of the equation we have the contribution of the valence electron \mathbf{k}_{\parallel}^v and the primary electron \mathbf{k}_{\parallel}^p , while on the right side the contribution of the detected electrons \mathbf{k}_{\parallel}^l (“left”) and \mathbf{k}_{\parallel}^r (“right”) can be found. The sum of these two terms is called sum momentum $\mathbf{k}_{\parallel}^{\text{sum}}$. Since we operate with a normal incidence primary beam we have $\mathbf{k}_{\parallel}^p = 0$. We note that $\mathbf{k}_{\parallel}^{\text{sum}}$ determines the value of the valence electron \mathbf{k}_{\parallel}^v . Since energy conservation has to hold the energy of the emitted electrons specify the binding energy of the valence electron. Therefore the position of the valence electron within the band structure is uniquely defined.

In order to disentangle exchange and correlation contributions, it is important, as will be described later in detail, to find a position with a high density of valence electron states of mainly one spin type. To this end we have calculated the electronic structure of the ground state of a thick Fe(001) film by means of an *ab initio* full-potential linear augmented-plane-wave (FLAPW) method [12]. The resulting spin- and layer-resolved densities of states reveal a strong predominance of majority spin for $\mathbf{k}_{\parallel}^v = 0$ and $E = -0.8$ eV.

Further, we calculated (e , $2e$) spectra with the aims of a quantitative comparison with our experimental spectra and of resolving them with respect to the valence electron spins. For these calculations we used a formalism, which has previously been presented in detail [7,8]. We therefore briefly recall only the concepts and expressions which are most essential for the present purpose. The central ingredients are matrix elements of the form

$$f^{\sigma\tau} = \langle l^{\sigma} r^{\tau} | U | p^{\sigma} \rangle | v^{\tau} \rangle, \quad (2)$$

where $|p^{\sigma}\rangle$ and $|v^{\tau}\rangle$ are the (spin-dependent) spatial parts of the primary and the valence electron states with spin orientations $\sigma = \pm$ and $\tau = \pm$ relative to the majority spin axis of the target. U denotes the screened Coulomb interaction. The two detected electrons are described by an antisymmetric two-electron state, the direct spatial part of which is

$$|l^{\sigma} r^{\tau}\rangle = |l^{\sigma}\rangle |r^{\tau}\rangle F_{\text{corr}}(\mathbf{k}, \mathbf{r}), \quad (3)$$

where $|l^{\sigma}\rangle$ and $|r^{\tau}\rangle$ are the spatial parts of time-reversed LEED states. These are coupled by the Coulomb correlation factor $F_{\text{corr}}(\mathbf{k}, \mathbf{r})$, which is a function of the relative momentum \mathbf{k} and the relative coordinate \mathbf{r} obtained as the numerical solution of a relative-particle Schrödinger equation involving U [8]. Because of the antisymmetry of the two-electron states we have, in addition to the direct matrix element $f^{\sigma\tau}$ [cf. Eq. (2)], an exchange matrix element $g^{\sigma\tau}$ which is analogous to $f^{\sigma\tau}$, with l^{σ} and r^{τ} interchanged.

For the cases spin σ of the primary electron parallel and antiparallel to the spin τ of the valence electron, i.e., $\tau = \sigma$ and $\tau = -\sigma = \bar{\sigma}$, we then have the fully spin-resolved (e , $2e$) reaction cross sections

$$I^{\sigma\sigma} \propto |f^{\sigma\sigma} - g^{\sigma\sigma}|^2 \delta \quad \text{and} \quad I^{\sigma\bar{\sigma}} \propto (|f^{\sigma\bar{\sigma}}|^2 + |g^{\sigma\bar{\sigma}}|^2) \delta, \quad (4)$$

where δ symbolizes the conservation of energy and surface-parallel momentum. From these partial intensities, summation over the valence electron spins yields the experimentally observable intensities

$$I^+ = I^{++} + I^{+-} \text{ for primary electron spin-up,} \quad (5a)$$

$$I^- = I^{-+} + I^{--} \text{ for primary electron spin-down.} \quad (5b)$$

For the application of the above (e , $2e$) formalism to Fe(001) we constructed from our ground state spin densities spin-dependent effective quasiparticle potentials.

These contain, in particular, spin-dependent imaginary self-energy parts V_{im}^{σ} , with $\sigma = +$ for spin-up and $\sigma = -$ for spin-down electrons. For the valence electron, V_{im}^{σ} was taken from a many-body calculation [13]. For the primary electron and the two detected electrons, which are represented by LEED states, we used the form $V_{\text{im}}^{\sigma} = a^{\sigma}(E + b^{\sigma})e^{c^{\sigma}}$, where $a^{+} = -0.22$, $b^{+} = 2.67$, $c^{+} = 0.69$, $a^{-} = -0.33$, $b^{-} = 4.67$, $c^{-} = 0.62$, and E is the kinetic energy. This choice is in quantitative accordance with experimental mean-free path data, which show that spin-down electrons are more strongly damped than spin-up electrons [14–16]. Using the above V_{im}^{σ} in a spin-dependent LEED calculation from Fe(001), we obtained the best agreement with experimental data [17]. In our present (e , $2e$) calculations, this V_{im}^{σ} yields significantly better agreement with our experimental data than a spin-independent V_{im} .

For the electron-electron interaction U in Eq. (2) we used a screened Coulomb potential in the Thomas-Fermi approximation $U \propto \exp(-r/\lambda)/r$ with the screening length as a parameter determined as $\lambda = 2.65 \text{ \AA}$ by comparing, for several primary energies, calculated (e , $2e$) spectra with their experimental counterparts.

Our aim is to disentangle exchange and correlation which requires a valence state of high spin polarization. From theory we know that the choice of $\mathbf{k}_{\parallel}^{\text{sum}} = 0$ and a binding energy 0.8 eV below the Fermi level E_F fulfills this. Experimentally, we allow $|\mathbf{k}_{\parallel}^{\text{sum}}| \leq 0.16 \text{ \AA}^{-1}$ in order to have sufficient statistics. Further, the symmetry of the experiment suggests to select those coincidence events, where the kinetic energy of both emitted electrons is equal. A primary energy of 25 eV demands both emitted electrons have a mean energy of 9.7 eV in order to access the selected valence state. For statistics reasons the energy sum of these two electrons has a window of 1 eV. For 2D momentum distributions of the data we note that for each coincident event the in-plane components of electron left and right are known. According to our coordinate system k_x^l is always negative while k_x^r is positive. Therefore, a coincidence event has an entry on the left and right half of the plot. In contrast to theory which covers the full momentum space the experiment has a limited range. Only momenta which fall inside the area, which has the solid lines as boundary, can be recorded; see Figs. 2(a) and 2(b). Let us discuss the experimental intensities I^{+} and I^{-} shown in panels (a) and (b). Starting at $|k_x^{l,r}| = 0$ we note that the coincidence intensity is zero which is purely instrumental since there is a gap between the detectors. Outside this “blind” region, starting at about $|k_x^{l,r}| = 0.2 \text{ \AA}^{-1}$, we observe an increase of the coincidence intensity for increasing k values. A maximum is reached at $|k_x^{l,r}| 0.7 \text{ \AA}^{-1}$. This reduced intensity for small $|k_x^{l,r}|$ values is a manifestation of the xc hole as shown previously in experiment and theory [4–6,8]. Apart from this similarity important differences between I^{+} and I^{-} can be noticed. First, the integrated intensity for I^{+} is higher than for I^{-} . Second, the

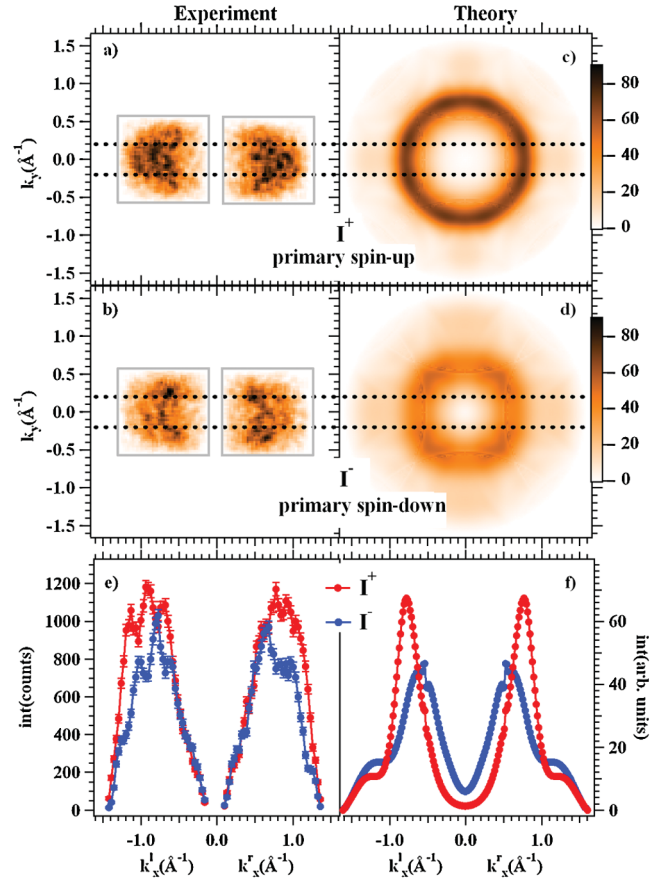


FIG. 2 (color). Results for excitation with a primary energy of 25 eV and emission of 9.7 eV electrons. In panels (a) and (c) the spin polarization of the primary beam and spin direction of the majority electrons are parallel (I^{+}), while they are antiparallel (I^{-}) in panels (b) and (d). Only momenta which fall inside the area which has the solid lines as boundary can be measured. Panels (e) and (f) are line scans through the distributions I^{+} and I^{-} with an integration width determined by the dashed lines in the upper panels.

intensity distribution for I^{+} is very different from I^{-} . Intensities of I^{-} close to the maximum value are confined to $|k_x^{l,r}|$ values near 0.7 \AA^{-1} . For I^{+} the intensity levels are close to the maximum value up to $|k_x^{l,r}|$ of 1.1 \AA^{-1} , before a drop can be observed. This is a consequence of the finite angular acceptance of the instrument.

Experimental and theoretical data are best compared via line scans through the 2D-momentum distributions for I^{+} and I^{-} , respectively, Figs. 2(e) and 2(f). The integration range along $|k_y^{l,r}|$ is indicated by the dashed horizontal lines in Fig. 2. Both experiment and theory clearly show that the maximum intensity for I^{+} is larger than the corresponding maximum for I^{-} . Further agreement consists in the larger extension of the depletion zone for I^{+} . The pair distributions in Fig. 2 contain, for each primary electron spin direction, collision events with both a majority- and a minority-spin valence electron according to Eq. (5). Further insight is obtained by considering these two events separately. To this end we show in Fig. 3 the calculated four

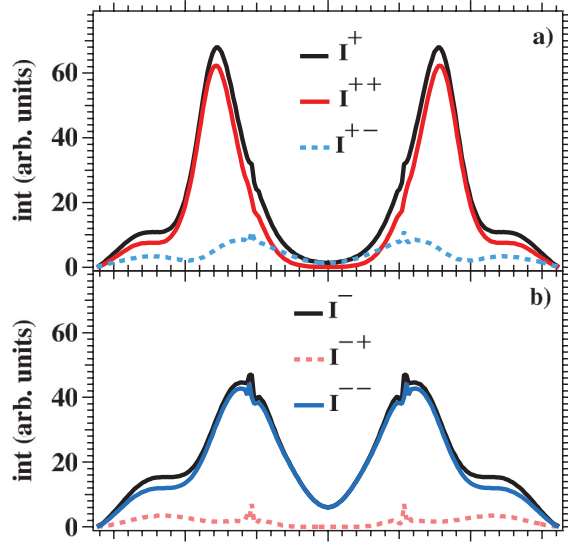


FIG. 3 (color). Spin-dependent intensities as calculated for the surface-parallel momentum along the [100] direction [Fig. 2(f)] cf. Eq. (5). (a) The solid red line shows the intensity of I^{++} (primary spin-up and valence electron spin-up). The dotted blue line relates to the intensity I^{+-} (primary spin-up and valence electron spin-down). The solid black line represents the sum of $I^{++} + I^{+-} = I^+$. (b) The solid blue line shows the intensity of I^{-+} (primary spin-down and valence electron spin-up). The dotted red line relates to the intensity I^{--} (primary spin-down and valence electron spin-down). The solid black line represents the sum of $I^{-+} + I^{--} = I^-$.

fully spin-resolved intensities $I^{\sigma\sigma}$ and $I^{\sigma\bar{\sigma}}$ [cf. Eq. (4)]. In Fig. 3(a) we show the decomposition of I^+ according to Eq. (5). We note that the main intensity to I^+ comes from the term I^{++} (primary spin-up and valence electron spin-up), whereas the term I^{+-} (primary spin-up and valence electron spin-down) is almost negligible. In other words: the intensity I^+ contains essentially only those collision events, where the spins of the primary and collision partner are parallel. Therefore exchange and correlation play a role. In a similar way the intensity I^- is mainly given by the contribution I^{-+} (primary spin-down and valence electron spin-up); see Fig. 3(b). Again, one can rephrase this by saying that the spin of the collision partner is antiparallel to the spin of the primary and only correlation is important. The origin of this spin selection is that the chosen valence state is essentially of majority type. This intrinsic spin resolution has an important consequence, namely, the possibility to separate exchange and correlation effects between the two outgoing electrons. For the parallel spin case $I^{++} \approx I^+$ both exchange and Coulomb correlation deter-

mine the size of the depletion zone, whereas for the anti-parallel spin case $I^{-+} \approx I^-$ only the correlation plays a role. The size of the depletion zone for I^+ is larger than for I^- . Therefore, one can say that the size of the exchange depletion zone has to exceed the size of the correlation depletion zone.

In summary, we have demonstrated by experimental and theoretical analysis that it is possible to identify the different contributions of exchange and Coulomb interaction to the size of the depletion zone observed in spin-dependent electron pair emission. Since this zone is closely related to the spin-dependent pair correlation function, our results also apply to the latter and thereby to the spin-dependent parts of the exchange-correlation hole.

We acknowledge the expert assistance of H. Engelhard and D. Hartung in designing and building the experimental apparatus.

-
- [1] E. Wigner and F. Seitz, Phys. Rev. **43**, 804 (1933).
 - [2] J. C. Slater, Rev. Mod. Phys. **6**, 209 (1934).
 - [3] J. Berakdar, H. Gollisch, and R. Feder, Solid State Commun. **112**, 587 (1999).
 - [4] N. Fominykh, J. Berakdar, J. Henk, and P. Bruno, Phys. Rev. Lett. **89**, 086402 (2002).
 - [5] F. O. Schumann, J. Kirschner, and J. Berakdar, Phys. Rev. Lett. **95**, 117601 (2005).
 - [6] F. O. Schumann, C. Winkler, and J. Kirschner, Phys. Rev. Lett. **98**, 257604 (2007).
 - [7] H. Gollisch and R. Feder, J. Phys. Condens. Matter **16**, 2207 (2004).
 - [8] H. Gollisch, N. v. Schwartzberg, and R. Feder, Phys. Rev. B **74**, 075407 (2006).
 - [9] D. T. Pierce and F. Meier, Phys. Rev. B **13**, 5484 (1976).
 - [10] S. Samarin, J. Berakdar, O. M. Artamonov, and J. Kirschner, Phys. Rev. Lett. **85**, 1746 (2000).
 - [11] A. Morozov, J. Berakdar, S. N. Samarin, F. U. Hillebrecht, and J. Kirschner, Phys. Rev. B **65**, 104425 (2002).
 - [12] See www.flapw.de.
 - [13] L. Chioncel, L. Vitos, I. A. Abrikosov, J. Kollár, M. I. Katsnelson, and A. I. Lichtenstein, Phys. Rev. B **67**, 235106 (2003).
 - [14] M. Getzlaff, J. Bansmann, and G. Schönhense, Solid State Commun. **87**, 467 (1993).
 - [15] D. P. Pappas, K. P. Kämper, B. P. Miller, H. Hopster, D. E. Fowler, C. R. Brundle, A. C. Luntz, and Z. X. Shen, Phys. Rev. Lett. **66**, 504 (1991).
 - [16] F. Passek, M. Donath, and K. Ertl, J. Magn. Magn. Mater. **159**, 103 (1996).
 - [17] R. Bertacco and F. Ciccacci, Phys. Rev. B **59**, 4207 (1999).